Decentralized Linear Motion Estimators for AUV Formations ⋆

Daniel Viegas Pedro Batista Paulo Oliveira Carlos Silvestre

Institute for Systems and Robotics, Instituto Superior Técnico
Av. Rovisco Pais, 1049-001 Lisboa, Portugal
{*dviegas,pbatista,pjcro,cjs*}*@isr.ist.utl.pt*

Abstract: This paper addresses the problem of decentralized state estimation in formations of Autonomous Underwater Vehicles (AUVs). In the envisioned scenario, each AUV in the formation estimates its own state relying only on locally available measurements and data communicated by neighboring agents, requiring lower computational and communication loads than centralized solutions. A method for designing local state observers featuring global error dynamics that converge asymptotically to zero is detailed, and an algorithm for improving its performance under stochastic disturbances and Gaussian uncertainties is presented. The proposed algorithm aims to minimize the H_2 norm of the global estimation error dynamics, expressed as an optimization problem subject to Bilinear Matrix Inequality (BMI) constraints. To assess the performance of the solution, realistic simulation results are presented and discussed for several formation topologies.

Keywords: Marine system navigation, guidance and control; Cooperative navigation; Navigation.

1. INTRODUCTION

The increasing use of formations in robotics, as well as the evolution of parallel computing, have led to extensive research on the field of distributed systems and agent formations, see e.g. Barooah (2007), Fax (2002), Tsitsiklis (1984), Middleton, R.H. and Braslavsky, J.H. (2010), and Sousa et al. (2009). In short, a distributed system consists of multiple autonomous computers or agents that communicate information between them and work towards a common goal.

There are many applications where the use of multiple agents in a cooperative setting is beneficial or even crucial. Unmanned Aerial Vehicles (UAVs) can be used in a formation setting advantageously, as close formation flight allows for reduced drag, thus allowing for more efficient fuel usage, see Giulietti et al. (2000) and Wolfe et al. (1996). In underwater applications, the concerted operation of formations of Autonomous Underwater Vehicles (AUVs) has many potential applications, such as minesweeping and oceanographic sampling, see Healey (2001) and Curtin et al. (1993). Automated highway systems also pose several problems related to formations, such as collision avoidance and traffic flow control, see Bender (1991) and Yanakiev and Kanellakopoulos (1996). In general, any task where a single agent is too slow or does not offer enough coverage, and any setting where multiple autonomous agents are present, may benefit from the study of the problem under a distributed point of view. One might wonder why the problems related with formations should be treated in a distributed setting when their treatment in a global, centralized way might probably be much simpler conceptually. However, the computations involved with large formations are often very heavy and would require much higher processing power of the agents, which is a problem when dealing with size and energy concerns, and would need the extensive use of telecommunications to and from a central processing node. Alternatively, a central computer could perform all the computations and spread them through the formation by communication, but it could cause unacceptable delays and communication loads.

This paper addresses the problem of state estimation in a formation of vehicles in a distributed setting. Each agent in the formation aims to estimate its own position based on some awareness of its own movement and local measurements and communications. In the specific case treated in this paper, each agent has access to either measurements of its absolute position, or measurements of its position relative to one or more agents as well as the state estimates of those agents, received through communication. Additionally, awareness of its own movement is provided by a measure of its linear acceleration, provided by an accelerometer mounted on-board. This problem is specially relevant in the scenario of a formation of AUVs working underwater, as sophisticated navigation solutions such as the Global Position System (GPS) are impractical due to the attenuation of electromagnetic waves in water. In this setting, one or more agents could have access to measurements of their absolute position using, e.g., range readings to a fixed source or to a series of beacons, see Batista et al. (2009b) and Batista et al. (2010). The other

⋆ This work was partially supported by Fundação para a Ciência e a Tecnologia (ISR/IST plurianual funding) through the PIDDAC Program funds, by the project PTDC/MAR/64546/2006 - OBSERVFLY of the FCT, and by the EU Project TRIDENT (Contract No. 248497).

agents would then rely on locally available measurements and data communication to estimate their own position. A method for local state observer design, rooted in classical state observer theory, is presented here, and the estimation error of the distributed state observer composed by the local estimators implemented in each agent of the formation is shown to converge globally asymptotically to zero for a certain class of formation structures. Namely, in the structures first considered there is no communication feedback between the agents, that is, the information flows in a single direction, and this allows for the calibration of the local observers based only on local dynamics, and without considering the specific shape of the formation. Building on this, an iterative algorithm, inspired by the $\mathcal{P}-\mathcal{K}$ iterations used in some controller synthesis problems, see Fransson and Lennartson (2003), is presented for improving the performance of such a decentralized observer in noisy environments, as well as constructively incorporating additional measurements and communication that may create information loops in the formation, based on the minimization of the H_2 norm of the estimation error dynamics. This problem is formulated as an optimization problem with bilinear matrix inequality (BMI) constraints.

The paper is organized as follows: Section 2 introduces the dynamics of the agents and of the local state observers, while Section 3 analyzes the convergence properties of the distributed state observer formed by the simultaneous implementation of local state observers by each agent in a formation. Section 4 formulates the problem of optimal decentralized state estimation as an optimization problem with BMI constraints, and presents an iterative algorithm to improve the performance of the decentralized state observer. Finally, Section 5 shows the results of several simulations carried out to assess the performance of the proposed solution.

1.1 Notation

Throughout the paper the symbol $\mathbf{0}$ denotes a matrix (or vector) of zeros and $\mathbf{I}$ an identity matrix, both of appropriate dimensions. Whenever relevant, the dimensions of an $n \times n$ identity matrix are indicated as $\mathbf{I}_n$. A block diagonal matrix is represented as $\text{diag}\,(\mathbf{A}_1, \ldots, \mathbf{A}_n)$, and the Kronecker product of two matrices $\mathbf{A}$ and $\mathbf{B}$ is denoted by $\mathbf{A}\otimes\mathbf{B}$. For $\mathbf{x}, \mathbf{y} \in \mathbb{R}^3$, $\mathbf{x}\times\mathbf{y}$ represents the cross product.

2. AGENT AND LOCAL STATE OBSERVER DYNAMICS

Consider a formation composed by N point-mass agents moving in a scenario, where each agent is identified by a distinct positive integer $i \in \{1, 2, \ldots, N\}$. Let $\{I\}$ denote an inertial reference coordinate frame and $\{B_i\}$ a coordinate frame attached to agent i, denominated in the sequel as the body-fixed coordinate frame associated with the i-th agent. The linear motion of agent i can be written as

$$\dot{\mathbf{p}}_i(t) = \mathbf{R}_i(t)\mathbf{v}_i(t), \tag{1}$$

where $\mathbf{p}_i(t) \in \mathbb{R}^3$ is the inertial position of the agent, $\mathbf{v}_i(t) \in \mathbb{R}^3$ denotes its velocity relative to $\{I\}$, and $\mathbf{R}_i(t) \in SO(3)$ is the rotation matrix from $\{B_i\}$ to $\{I\}$, which satisfies

$$\dot{\mathbf{R}}_i(t) = \mathbf{R}_i(t)\mathbf{S}(\boldsymbol{\omega}_i(t)),$$

where $\boldsymbol{\omega}_i(t) \in \mathbb{R}^3$ is the angular velocity of $\{B_i\}$, expressed in body-fixed coordinates, and $\mathbf{S}(\boldsymbol{\omega})$ is the skew-symmetric matrix such that $\mathbf{S}(\boldsymbol{\omega})\boldsymbol{x}$ is the cross product $\boldsymbol{\omega} \times \boldsymbol{x}$. It is assumed that an Attitude and Heading Reference System (AHRS) installed on-board each agent provides measurements of both $\mathbf{R}_i(t)$ and $\boldsymbol{\omega}_i(t)$. Additionally, suppose that each agent has access to a linear acceleration measurement $\mathbf{a}_i(t) \in \mathbb{R}^3$, which follows

$$\mathbf{a}_i(t) = \dot{\mathbf{v}}_i(t) + \mathbf{S}(\boldsymbol{\omega}_i(t))\mathbf{v}_i(t) - \mathbf{g}_i(t), \tag{2}$$

where $\mathbf{g}_i(t) \in \mathbb{R}^3$ is the acceleration of gravity, expressed in body-fixed coordinates. Even though the acceleration of gravity is usually well-known, it is treated as an unknown variable with practical applications in mind, where small errors in the estimation of the attitude of the agent may lead to significant errors in the acceleration compensation. Its time derivative is given by

$$\dot{\mathbf{g}}_i(t) = -\mathbf{S}(\boldsymbol{\omega}_i(t))\mathbf{g}_i(t). \tag{3}$$

Finally, consider that each agent has access to either:

(1) a measurement of its own inertial position, provided by a GPS or by an Ultra-short Baseline (USBL) positioning system; or
(2) measurements of its position relative to one or more agents in the vicinity, denoted in the sequel as the source-agents of agent i,

$$\Delta\mathbf{p}_i(t) := \begin{bmatrix} \mathbf{p}_i(t) - \mathbf{p}_{a_{i,1}}(t) \\ \mathbf{p}_i(t) - \mathbf{p}_{a_{i,2}}(t) \\ \vdots \\ \mathbf{p}_i(t) - \mathbf{p}_{a_{i,N_i}}(t) \end{bmatrix} \in \mathbb{R}^{3N_i}, a_{i,j} \in \mathcal{A}_i, \tag{4}$$

where

$$\mathcal{A}_i := \{a_{i,1}, a_{i,2}, \ldots, a_{i,N_i} | \\ a_{i,j} \in \{1, \ldots, N\}, j = 1, \ldots, N_i\}$$

is the set of source-agents of agent i, and N_i the number of source-agents of agent i. Furthermore, each of those agents transmits its own position estimate $\hat{\mathbf{p}}_{a_{i,j}}(t) \in \mathbb{R}^3$ to agent i.

Now, consider the problem of decentralized state estimation in the formation, in the sense that each agent aims to estimate its inertial position using only locally available data, that is, measurements provided by the on-board sensor-suite and position estimates received from its source-agents. For the first case, i.e., with absolute position readings, grouping equations (1) through (3), and measuring the absolute position, yields the system

$$\begin{cases} \dot{\mathbf{p}}_i(t) = \mathbf{R}_i(t)\mathbf{v}_i(t) \\ \dot{\mathbf{v}}_i(t) = -\mathbf{S}(\boldsymbol{\omega}_i(t))\mathbf{v}_i(t) + \mathbf{g}_i(t) + \mathbf{a}_i(t) \\ \dot{\mathbf{g}}_i(t) = -\mathbf{S}(\boldsymbol{\omega}_i(t))\mathbf{g}_i(t) \\ \mathbf{y}_i(t) = \mathbf{p}_i(t) \end{cases}. \tag{5}$$

Using in each vehicle the Lyapunov state transformation introduced in Batista et al. (2009a),

$$\begin{bmatrix} \mathbf{x}_i^1(t) \\ \mathbf{x}_i^2(t) \\ \mathbf{x}_i^3(t) \end{bmatrix} := \begin{bmatrix} \mathbf{I} & \mathbf{0} & \mathbf{0} \\ \mathbf{0} & \mathbf{R}_i(t) & \mathbf{0} \\ \mathbf{0} & \mathbf{0} & \mathbf{R}_i(t) \end{bmatrix} \begin{bmatrix} \mathbf{p}_i(t) \\ \mathbf{v}_i(t) \\ \mathbf{g}_i(t) \end{bmatrix}, \tag{6}$$

which preserves stability and observability properties, and making $\mathbf{u}_i(t) := \mathbf{R}_i(t)\mathbf{a}_i(t)$, the system dynamics can be written as the linear time-invariant (LTI) system

$$\begin{cases} \dot{\mathbf{x}}_i(t) = \mathbf{A}_L\mathbf{x}_i(t) + \mathbf{B}_L\mathbf{u}_i(t) \\ \mathbf{y}_i(t) = \mathbf{C}_L\mathbf{x}_i(t) \end{cases}, \tag{7}$$

where $\mathbf{x}_i^T(t) = \left[[\mathbf{x}_i^1(t)]^T \ [\mathbf{x}_i^2(t)]^T \ [\mathbf{x}_i^3(t)]^T\right]^T \in \mathbb{R}^n$, $n = 9$, is the state of the system,

$$\mathbf{A}_L = \begin{bmatrix} \mathbf{0} & \mathbf{I} & \mathbf{0} \\ \mathbf{0} & \mathbf{0} & \mathbf{I} \\ \mathbf{0} & \mathbf{0} & \mathbf{0} \end{bmatrix}, \ \mathbf{B}_L = \begin{bmatrix} \mathbf{0} \\ \mathbf{I} \\ \mathbf{0} \end{bmatrix}, \text{ and } \mathbf{C}_L = [\mathbf{I} \ \mathbf{0} \ \mathbf{0}].$$

Simple calculations show that the pair $(\mathbf{A}_L, \mathbf{C}_L)$ is observable, thus it is straightforward to design a local state observer for agent i with globally asymptotically stable error dynamics, see Astrom and Murray (2008).

For the second case, i.e., when the agent has access to relative position measurements, grouping equations (1) through (3) and taking the relative position measurements (4) as the output yields the system

$$\begin{cases} \dot{\mathbf{p}}_i(t) = \mathbf{R}_i(t)\mathbf{v}_i(t) \\ \dot{\mathbf{v}}_i(t) = -\mathbf{S}(\boldsymbol{\omega}_i(t))\mathbf{v}_i(t) + \mathbf{g}_i(t) + \mathbf{a}_i(t) \\ \dot{\mathbf{g}}_i(t) = -\mathbf{S}(\boldsymbol{\omega}_i(t))\mathbf{g}_i(t) \\ \mathbf{y}_i(t) = \Delta\mathbf{p}_i(t) \end{cases}, \tag{8}$$

and applying (6) yields the compact form

$$\begin{cases} \dot{\mathbf{x}}_i(t) = \mathbf{A}_L\mathbf{x}_i(t) + \mathbf{B}_L\mathbf{u}_i(t) \\ \mathbf{y}_i(t) = \mathbf{C}_i\Delta\mathbf{x}_i(t) \end{cases}, \tag{9}$$

where $\mathbf{x}_i(t)$, $\mathbf{A}_L$, and $\mathbf{B}_L$ are defined as in (7), $\mathbf{C}_i = \left[\mathbf{C}_L^T \ \mathbf{C}_L^T \ \dots \ \mathbf{C}_L^T\right]^T \in \mathbb{R}^{3N_i \times nN_i}$, and

$$\Delta\mathbf{x}_i(t) := \begin{bmatrix} \mathbf{x}_i(t) - \mathbf{x}_{a_{i,1}}(t) \\ \mathbf{x}_i(t) - \mathbf{x}_{a_{i,2}}(t) \\ \vdots \\ \mathbf{x}_i(t) - \mathbf{x}_{a_{i,N_i}}(t) \end{bmatrix} \in \mathbb{R}^{nN_i}. \tag{10}$$

The above system resembles the usual representation of LTI systems, the key difference being that the measurements on the system depends on the state of another agents. As such, the dynamics of the local state observers are defined as

$$\begin{cases} \dot{\hat{\mathbf{x}}}_i(t) := \mathbf{A}_L\hat{\mathbf{x}}_i(t) + \mathbf{B}_L\mathbf{u}_i(t) + \mathbf{L}_i(\mathbf{y}_i(t) - \hat{\mathbf{y}}_i(t)) \\ \hat{\mathbf{y}}_i(t) := \mathbf{C}_i\Delta\hat{\mathbf{x}}(t) \end{cases}, \tag{11}$$

where $\hat{\mathbf{x}}_i(t) \in \mathbb{R}^n$ is the state estimate of agent i, $\mathbf{L}_i \in \mathbb{R}^{n \times 3N_i}$ is an arbitrary matrix of output feedback weights, to be determined, and

$$\Delta\hat{\mathbf{x}}_i(t) := \begin{bmatrix} \hat{\mathbf{x}}_i(t) - \hat{\mathbf{x}}_{a_{i,1}}(t) \\ \hat{\mathbf{x}}_i(t) - \hat{\mathbf{x}}_{a_{i,2}}(t) \\ \vdots \\ \hat{\mathbf{x}}_i(t) - \hat{\mathbf{x}}_{a_{i,N_i}}(t) \end{bmatrix} \in \mathbb{R}^{nN_i}. \tag{12}$$

Defining the estimation error of agent i, $\tilde{\mathbf{x}}_i(t) \in \mathbb{R}^n$ as

$$\tilde{\mathbf{x}}_i(t) := \mathbf{x}_i(t) - \hat{\mathbf{x}}_i(t),$$

the estimation error of its j-th source-agent $\tilde{\mathbf{x}}_{a_{i,j}}(t) \in \mathbb{R}^n$ as

$$\tilde{\mathbf{x}}_{a_{i,j}}(t) := \mathbf{x}_{a_{i,j}}(t) - \hat{\mathbf{x}}_{a_{i,j}}(t),$$

and splitting $\mathbf{L}_i$ into the blocks referring to each of the N_i distinct measurements,

$$\mathbf{L}_i = \left[\mathbf{L}_i^{a_{i,1}} \ \mathbf{L}_i^{a_{i,2}} \ \dots \ \mathbf{L}_i^{a_{i,N_i}}\right], \mathbf{L}_i^{a_{i,j}} \in \mathbb{R}^{n \times 3},$$

the error dynamics can be written as

$$\dot{\tilde{\mathbf{x}}}_i(t) = \left(\mathbf{A}_L - \sum_{k=1}^{N_i} \mathbf{L}_i^{a_{i,k}}\mathbf{C}_L\right)\tilde{\mathbf{x}}_i(t) + \sum_{k=1}^{N_i} \mathbf{L}_i^{a_{i,k}}\mathbf{C}_L\tilde{\mathbf{x}}_{a_{i,k}}(t). \tag{13}$$

Remark 1. It is possible to consider a third case of agents that would receive both absolute and relative position measurements. This is straightforward and therefore, for the sake of clarity of presentation, it is not considered in this paper.

3. STABLE OBSERVER GAINS

This section presents a sufficient condition for global asymptotic stability of the error of the decentralized state observer presented in the previous section. Agent formations such as the one considered in this paper can be handily described by a directed graph, and as such it is convenient to introduce some concepts on graph theory, see Wallis (2007) and West (2001).

A directed graph, or digraph, $\mathcal{G} := (\mathcal{V}, \mathcal{E})$ is composed by a set $\mathcal{V}$ of vertices together with a set of directed edges $\mathcal{E}$, which are ordered pairs of vertices. Such an edge can be expressed as $e = (a, b)$, meaning that edge e is incident on vertices a and b, directed towards b. A directed path in $\mathcal{G}$ is a sequence $(v_0, e_1, v_1, e_2, v_2, \dots, e_n, v_n)$ of distinct vertices (with the possible exception of the first and the last) and edges of $\mathcal{G}$ such that $e_i = (v_{i-1}, v_i)$. A directed cycle is a directed path in which the first and the last vertices are the same. A directed graph is called acyclic if it contains no directed cycles.

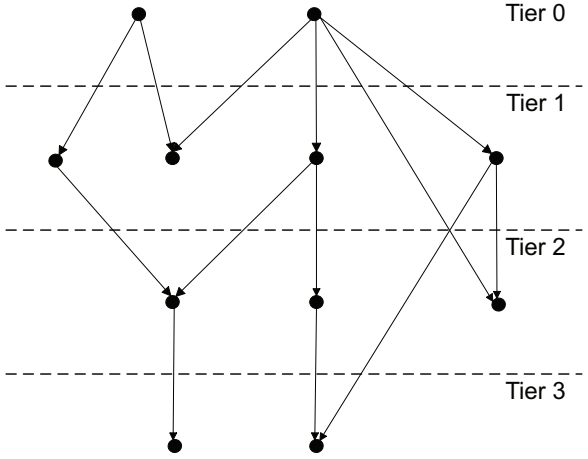

Fig. 1. Drawing of an acyclic directed graph divided in tiers

If a directed graph $\mathcal{G}$ is acyclic, it can be represented graphically by a tiered drawing such as the one depicted in Fig. 1, that is, the drawing is divided in K hierarchical tiers following a few simple rules: tier 0 is composed of the vertices with no edges directed towards them while, for a vertex in tier $k > 0$, all directed paths ending in that vertex start in a node of a lower tier. In this paper, each vertex is denoted by its tier k and an identifier i in the respective tier (e.g., some quantity x associated with vertex 4 in tier 2 is denoted as $x_{2/4}$, and the vertex itself is identified as $\{2/4\}$). Furthermore, the number of vertices in a given tier k is denoted by T_k.

Now, consider the agent formation described in the previous section. This kind of formation can be associated with a directed graph $\mathcal{G} = (\mathcal{V}, \mathcal{E})$, where each vertex represents a distinct agent, and an edge (a, b) means that agent a is a source-agent of agent b. Note that the vertices with no edges directed towards them refer to agents with access to measurements of their own absolute position.

The following result establishes a sufficient condition for global asymptotic stability of the estimation error for the distributed state observer.

Theorem 1. Consider a formation composed of N agents, whose dynamics are described either by (7) or (9), depending on the type of measurements available to them, and assume that the digraph associated with the formation is acyclic. Suppose that each agent $\{a/b\}$ described by (7) implements a local state observer with globally asymptotically stable error dynamics, with gain $\mathbf{L}_{a/b}$, and that each agent $\{k/i\}$ described by (9) implements the local state observer (11), with the gain $\mathbf{L}_{k/i}$ chosen so that the matrix $\left(\mathbf{A}_L - \sum_{j=1}^{N_{k/i}} \mathbf{L}_{k/i}^{a_{k/i,j}} \mathbf{C}_L\right)$ is stable. Then, the estimation error of the distributed state observer,

$$\mathbf{e}(t) := \begin{bmatrix} \tilde{\mathbf{x}}_{0/1}(t) \\ \tilde{\mathbf{x}}_{0/2}(t) \\ \vdots \\ \tilde{\mathbf{x}}_{K-1/T_{K-1}}(t) \end{bmatrix} \in \mathbb{R}^{nN},$$

composed by the concatenation of the estimation error of each local observer, converges globally assymptotically to zero, and its dynamics satisfy

$$\dot{\mathbf{e}}(t) = \mathbf{\Lambda}\mathbf{e}(t), \tag{14}$$

for some $\mathbf{\Lambda} \in \mathbb{R}^{nN \times nN}$, whose eigenvalues are those of each local state observer.

Proof. Since the graph $\mathcal{G} = (\mathcal{V}, \mathcal{E})$ associated with the formation is acyclic, consider its drawing with K tiers each with some number T_k of agents. Denote the estimation error of each local observer in a tier by $\tilde{\mathbf{x}}_{k/i}(t)$, where k is its tier and $i \in \{1, 2, \ldots, T_k\}$ corresponds to its identifier in the tier. Note that the dynamics of the local state observer of an agent in a given tier only depends on measurements from agents in lower tiers, allowing to study its properties regardless of the composition of higher tiers.

Since the agents in tier 0 have access to measurements of their absolute position, the global estimation error for that tier, $\mathbf{e}_0(t) := \left[[\tilde{\mathbf{x}}_{0/1}(t)]^T \; [\tilde{\mathbf{x}}_{0/2}(t)]^T \; \ldots \; [\tilde{\mathbf{x}}_{0/T_0}(t)]^T\right]$ satisfies

$$\dot{\mathbf{e}}_0(t) = \mathbf{\Lambda}_0 \mathbf{e}_0(t), \tag{15}$$

with

$$\mathbf{\Lambda}_0 = \text{diag}((\mathbf{A}_L - \mathbf{L}_{0/1}\mathbf{C}_L), (\mathbf{A}_L - \mathbf{L}_{0/2}\mathbf{C}_L), \ldots, (\mathbf{A}_L - \mathbf{L}_{1/T_0}\mathbf{C}_L)),$$

whose eigenvalues are those of each local observer in tier 0.

Taking any tier k, its error dynamics can be grouped with those of the lower tiers, yielding

$$\begin{bmatrix} \dot{\mathbf{e}}_{0,\ldots,k-1}(t) \\ \dot{\mathbf{e}}_k(t) \end{bmatrix} = \begin{bmatrix} \mathbf{K} & \mathbf{0} \\ \mathbf{\Psi}_k & \Lambda_k \end{bmatrix} \begin{bmatrix} \mathbf{e}_{0,\ldots,k-1}(t) \\ \mathbf{e}_k(t) \end{bmatrix}, \tag{16}$$

where $\mathbf{K}$ is the matrix representing the estimation error dynamics of tiers 0 through $k-1$,

$$\Lambda_k = \text{diag}\left[\left(\mathbf{A}_L - \sum_{j=1}^{N_{k/1}} \mathbf{L}_{k/1}^{a_{k/1,j}} \mathbf{C}_L\right), \left(\mathbf{A}_L - \sum_{j=1}^{N_{k/2}} \mathbf{L}_{k/2}^{a_{k/2,j}} \mathbf{C}_L\right), \ldots, \left(\mathbf{A}_L - \sum_{j=1}^{N_{k/T_k}} \mathbf{L}_{k/T_k}^{a_{k/T_k,j}} \mathbf{C}_L\right)\right] \tag{17}$$

is a stable matrix, whose eigenvalues are those of each local observer in tier k, and

$$\mathbf{\Psi}_k = \left[[\mathbf{\Psi}_{k/1}]^T \; [\mathbf{\Psi}_{k/2}]^T \; \ldots \; [\mathbf{\Psi}_{k/T_k}]^T\right]^T, \tag{18}$$

where

$$\mathbf{\Psi}_{k/i} = \left[\boldsymbol{\psi}_{k/i}(\{0/1\})\boldsymbol{\psi}_{k/i}(\{0/2\}) \ldots \boldsymbol{\psi}_{k/i}(\{k-1/T_{k-1}\})\right],$$

with

$$\boldsymbol{\psi}_{k/i}(\{a/b\}) = \begin{cases} \mathbf{L}_{k/i}^{a/b}\mathbf{C}_L, \; \{a/b\} \in \mathcal{A}_{k/i} \\ \mathbf{0}, \text{ otherwise} \end{cases}.$$

From (16), it is straightforward to show that the eigenvalues of the global error dynamics of tiers 0 through k are those of $\mathbf{K}$ and $\mathbf{\Lambda}_k$. Therefore, if the matrix representing the dynamics of the global estimation error of tiers 0 to $k-1$, $\mathbf{K}$, is stable, then the dynamics of the global estimation error of tiers 0 to k will also be stable, and the error will converge globally asymptotically to zero.
Since:

1) the distributed state estimator formed by all agents in tier 0 is stable, and the eigenvalues of the dynamics of its estimation error are those of each local observer in tier 0, and

2) the addition of tier k to the dynamics of the estimation error of the previous tiers yields new error dynamics whose eigenvalues are the same, plus the eigenvalues of the error dynamics of each state observer in tier k, it follows, by induction, that the dynamics of the global estimation error of the full formation satisfy (14). Then, since the matrix $\mathbf{L}_{k/i}$ of each state observer is chosen such that $\left(\mathbf{A}_L - \sum_{j=1}^{N_{k/i}} \mathbf{L}_{k/i}^{a_{k/i,j}} \mathbf{C}_L\right)$ is stable, the estimation error converges globally asymptotically to zero. □

This result allows the design of a distributed estimator in the terms described in Section 2. Note that the state observer of each agent can be designed locally.

Remark 2. It is also possible to use this method to design a stable state observer when the graph associated with the formation is cyclic, by removing edges from the graph until it is no longer cyclic, while making sure to never remove the last edge directed towards a vertex. This straightforward approach is then applied to the observers by zeroing the gains referring to edges which were removed during this process.

4. PERFORMANCE IN NOISY ENVIRONMENTS

The previous section presented a method for designing decentralized state observers for agent formations such as the one described in Section 1. While stability is assured, there are no guarantees regarding performance in noisy environments, which is critical in most practical settings. As such, this section introduces a method for improving the performance of the state observer in the presence of sensor noise and cycles in the graph associated with the structure of the formation.

4.1 Global Observer Dynamics

To study and improve the performance of the decentralized state observer, it is necessary to consider the global

dynamics of the formation, which can be represented in the LTI form

$$\begin{cases} \dot{\boldsymbol{x}}(t) = \mathbf{A}_g \boldsymbol{x}(t) + \mathbf{B}_g \boldsymbol{u}(t) + \mathbf{w}(t) \\ \boldsymbol{y}(t) = \mathbf{C}_g \boldsymbol{x}(t) + \mathbf{v}(t) \end{cases}, \tag{19}$$

where $\boldsymbol{x}(t) := \left[\mathbf{x}_1^T(t)\, \mathbf{x}_2^T(t) \ldots \mathbf{x}_N^T(t)\right]^T \in \mathbb{R}^{nN}$ is the state of the whole formation, $\boldsymbol{y}(t) := \left[\mathbf{y}_1^T(t)\, \mathbf{y}_2^T(t) \ldots \mathbf{y}_N^T(t)\right]^T \in \mathbb{R}^{3M}$ the output of the system, M being the total number of measurements in the whole formation, and $\boldsymbol{u}(t) := \left[\mathbf{u}_1^T(t)\ \mathbf{u}_2^T(t)\ \ldots\ \mathbf{u}_N^T(t)\right]^T \in \mathbb{R}^{3N}$ is the input of the system. The variables $\mathbf{w}(t) \in \mathbb{R}^{nN}$ and $\mathbf{v}(t) \in \mathbb{R}^{3M}$ represent, respectively, process and observation noise, which are assumed to be zero-mean uncorrelated white Gaussian processes, with associated covariance matrices $\mathbf{Q} \in \mathbb{R}^{nN \times nN}$ and $\mathbf{R} \in \mathbb{R}^{3M \times 3M}$. The matrices $\mathbf{A}_g \in \mathbb{R}^{nN \times nN}$ and $\mathbf{B}_g \in \mathbb{R}^{nN \times 3N}$ are built from the dynamics of the individual agents, following

$$\begin{cases} \mathbf{A}_g = \mathbf{I}_N \otimes \mathbf{A}_L \\ \mathbf{B}_g = \mathbf{I}_N \otimes \mathbf{B}_L \end{cases}. \tag{20}$$

To describe $\mathbf{C}_g \in \mathbb{R}^{3M \times nN}$, it is useful to build a matrix $\mathbf{S} \in \mathbb{R}^{N \times M}$ similar to the incidence matrix of graph $\mathcal{G}$. First, define virtual edges of the form $(0, i)$ to represent the absolute position measurements that are available to some of the agents, then build $\mathbf{S}$ the same way the incidence matrix would be built, that is, its individual entries follow

$$\mathbf{S}_{ij} = \begin{cases} 1, \text{ edge } j \text{ incident on } i, \text{ directed towards it,} \\ -1, \text{ edge } j \text{ incident on } i, \text{ directed away from it,} \\ 0, \text{ otherwise.} \end{cases} \tag{21}$$

Then, $\mathbf{C}_g$ follows

$$\mathbf{C}_g = \mathbf{S}^T \otimes \mathbf{C}_L.$$

The local state observers can also be grouped in a similar way, yielding

$$\begin{cases} \dot{\hat{\boldsymbol{x}}}(t) := \mathbf{A}_g \hat{\boldsymbol{x}}(t) + \mathbf{B}_g \boldsymbol{u}(t) + \mathbf{L}(\boldsymbol{y}(t) - \hat{\boldsymbol{y}}(t)) \\ \hat{\boldsymbol{y}}(t) := \mathbf{C}_g \hat{\boldsymbol{x}}(t) \end{cases}, \tag{22}$$

where $\hat{\boldsymbol{x}}(t) := \left[\hat{\mathbf{x}}_1^T(t)\, \hat{\mathbf{x}}_2^T(t) \ldots \hat{\mathbf{x}}_N^T(t)\right]^T \in \mathbb{R}^{nN}$ is the global state estimate of the decentralized state observer, and $\mathbf{L} \in \mathbb{R}^{nN \times 3M}$ is the matrix of observer gains. To account for the fact that each local observer only has access to some measurements, $\mathbf{L}$ must follow a special structure, or sparsity constraint. More specifically, define an augmented incidence matrix, $\mathbf{S}' \in \mathbb{R}^{nN \times 3M}$, as

$$\mathbf{S}' = \mathbf{S} \otimes \mathbf{1}_{n,3}, \tag{23}$$

where $\mathbf{1}_{n,m}$ is a $n \times m$ matrix whose entries are all equal to 1. Then, the individual entries of $\mathbf{L}$ follow

$$\begin{cases} \mathbf{S}'_{ij} = 1 \Rightarrow \mathbf{L}_{ij} \text{ can be set to an arbitrary value} \\ \mathbf{S}'_{ij} \neq 1 \Rightarrow \mathbf{L}_{ij} = 0. \end{cases}$$

This can be expressed as linear constraint for optimization purposes:

$$\mathbf{L}_{ij} = 0 \text{ if } \mathbf{S}'_{ij} \neq 1, \forall i \in \{1, 2, \ldots, nN\}, j \in \{1, 2, \ldots, 3M\}. \tag{24}$$

The sparsity constraint imposed on $\mathbf{L}$ prevents the use of classical filter design techniques such as the Kalman filter, and as such a different strategy must be pursued to find suitable observer gains.

4.2 H_2 Nominal Performance

Consider the system

$$\begin{cases} \dot{\mathbf{x}}(t) = \mathbf{A}\mathbf{x}(t) + \mathbf{B}\mathbf{u}(t) \\ \mathbf{z}(t) = \mathbf{C}\mathbf{x}(t) + \mathbf{D}\mathbf{u}(t) \end{cases}, \tag{25}$$

where $\mathbf{x}(t) \in \mathbb{R}^m$ is the state of the system, $\mathbf{u}(t) \in \mathbb{R}^o$ the input, and $\mathbf{z}(t) \in \mathbb{R}^p$ is the output. The matrices $\mathbf{A}$, $\mathbf{B}$, $\mathbf{C}$, and $\mathbf{D}$ are constant real matrices of appropriate dimensions. Denote the corresponding transfer function by $\mathbf{T}(s) = \mathbf{C}(\mathbf{I}s - \mathbf{A})^{-1}\mathbf{B} + \mathbf{D}$.

The H_2 norm of the system, $\|\mathbf{T}\|_{H_2}$, which verifies

$$\|\mathbf{T}\|_{H_2}^2 = \frac{1}{2\pi} \text{trace} \int_{-\infty}^{\infty} \mathbf{T}(j\omega)\mathbf{T}(j\omega)^* d\omega, \tag{26}$$

can be used as a performance metric for state observers. In fact, when the components of the input $\mathbf{u}(t)$ are independent zero-mean, white Gaussian noise processes, the $\mathbf{H}_2$ norm of the system is also the asymptotic output variance of the system, see Scherer and Weiland (2005). The global error of the decentralized state observer (22), $\tilde{\boldsymbol{x}}(t) \in \mathbb{R}^{nN}$, is defined as

$$\tilde{\boldsymbol{x}}(t) = \boldsymbol{x}(t) - \hat{\boldsymbol{x}}(t). \tag{27}$$

Taking its time derivative and using (19) and (22) yields

$$\dot{\tilde{\boldsymbol{x}}}(t) = (\mathbf{A}_g - \mathbf{L}\mathbf{C}_g)\tilde{\boldsymbol{e}}(t) + \mathbf{w}(t) - \mathbf{L}\mathbf{v}(t). \tag{28}$$

Define a zero-mean, uncorrelated, white Gaussian noise process $\mathbf{q}(t) \in \mathbb{R}^{nN+3M}$ whose covariance is the identity matrix. The error dynamics (28) can then be rewritten as

$$\dot{\tilde{\boldsymbol{x}}}(t) = (\mathbf{A}_g - \mathbf{L}\mathbf{C}_g)\tilde{\boldsymbol{x}}(t) + \left[\mathbf{Q}^{\frac{1}{2}}\ -\mathbf{L}\mathbf{R}^{\frac{1}{2}}\right]\mathbf{q}(t). \tag{29}$$

By making the substitution

$$\begin{cases} \mathbf{A} = (\mathbf{A}_g - \mathbf{L}\mathbf{C}_g), \\ \mathbf{B} = \left[\mathbf{Q}^{\frac{1}{2}}\ -\mathbf{L}\mathbf{R}^{\frac{1}{2}}\right], \\ \mathbf{C} = \mathbf{I}, \\ \mathbf{D} = \mathbf{0}, \\ \mathbf{x}(t) = \tilde{\boldsymbol{x}}(t), \\ \mathbf{u}(t) = \mathbf{q}(t), \end{cases} \tag{30}$$

the system (19) describes the error dynamics of the decentralized state observer, and its H_2 norm is also the asymptotic variance of the estimation error. Thus, the problem of optimizing the performance of the state observer in noisy environments can be restated as minimizing the H_2 norm of (19).

Consider the following result, resorting to Linear Matrix Inequality (LMI) concepts, as described in Scherer and Weiland (2005), presented here in a simplified form:

Theorem 2. Suppose that the system (19) is asymptotically stable. Then

(1) $\|\mathbf{T}\|_2 < \infty$ if and only if $\mathbf{D} = 0$.
(2) If $\mathbf{D} = 0$ then the following statements are equivalent:
   (a) $\|\mathbf{T}\|_2 < \gamma$.
   (b) there exists $\mathbf{P} = \mathbf{P}^T \succ \mathbf{0}$ and $\mathbf{Z}$ such that

$$\begin{bmatrix} \mathbf{A}^T\mathbf{P} + \mathbf{P}\mathbf{A} & \mathbf{P}\mathbf{B} \\ \mathbf{B}^T\mathbf{P} & -\gamma\mathbf{I} \end{bmatrix} \prec \mathbf{0}, \begin{bmatrix} \mathbf{P} & \mathbf{C}^T \\ \mathbf{C} & \mathbf{Z} \end{bmatrix} \succ \mathbf{0}, \quad \text{and } \text{trace}(\mathbf{Z}) < \gamma \tag{31}$$

Define

$$\mathbf{X}(\mathbf{P},\mathbf{L},\gamma) := \begin{bmatrix} (\mathbf{A}_g-\mathbf{L}\mathbf{C}_g)^T\mathbf{P}+\mathbf{P}(\mathbf{A}_g-\mathbf{L}\mathbf{C}_g) & \mathbf{P}\begin{bmatrix}\mathbf{Q}^{\frac{1}{2}} & -\mathbf{L}\mathbf{R}^{\frac{1}{2}}\end{bmatrix} \\ \begin{bmatrix}\mathbf{Q}^{\frac{1}{2}} & -\mathbf{L}\mathbf{R}^{\frac{1}{2}}\end{bmatrix}^T\mathbf{P} & -\gamma\mathbf{I} \end{bmatrix}$$

Using Theorem 2 and the substitution (30), the minimization of the H_2 norm can be done solving the optimization problem

$$\begin{aligned} \min_{\substack{\mathbf{P}\in\mathbb{R}^{nN\times nN}\\ \mathbf{L}\in\mathbb{R}^{nN\times 3M}\\ \mathbf{Z}\in\mathbb{R}^{nN\times nN}\\ \gamma\in\mathbb{R}^+}} \quad & \gamma \\ \text{subject to:} \quad & \mathbf{P}\succ\mathbf{0}, \\ & \mathbf{X}(\mathbf{P},\mathbf{L},\gamma)\prec 0, \\ & \begin{bmatrix}\mathbf{P} & \mathbf{I}\\ \mathbf{I} & \mathbf{Z}\end{bmatrix}\succ\mathbf{0}, \\ & \text{trace}(\mathbf{Z})<\gamma, \\ & \text{and } \mathbf{L}_{ij}=0 \text{ if } \mathbf{S}'_{ij}\neq 1, \\ & \forall i\in\{1,2,\ldots,nN\}, j\in\{1,2,\ldots,3M\}, \end{aligned} \tag{32}$$

see Scherer and Weiland (2005). The resulting set of constraints contains a BMI, which is inherently difficult to treat and is usually associated with nonconvex problems. In fact, even finding a feasible solution is a NP-hard problem, see Toker, O. and Ozbay, H. (1995). While it is possible, for centralized systems, to apply a variable substitution which renders the constraints linear, the structural constraint imposed on $\mathbf{L}$ in the decentralized case inviabilizes this approach. On the other hand, Theorem 1 allows to find stable observer gains, and as such provides a way to find a feasible set of variables for the constraints of (32). In fact, if the value of $\mathbf{L}$ is fixed, the constraints take a Linear Matrix Inequality (LMI) form, and there exist very fast and efficient methods to solve optimization problems with LMI constraints. Following this, Table 1 details an algorithm for improvement of the performance of the decentralized state observer, similar to the $\mathcal{P}-\mathcal{K}$ iterations used in some cases for controller design via BMIs, see Fransson and Lennartson (2003).

Note that there are no guarantees that the algorithm will find the optimal observer gains, or even that it will improve on the initial $\mathbf{L}$. However, there is the guarantee that γ will not increase over the run of the algorithm. In step 2 of the k-th iteration of the algorithm, solving (33) yields optimal γ and $\mathbf{P}^{(k)}$ for the given $\mathbf{L}^{(k-1)}$. Denote the values found for $\mathbf{Z}$ and γ, respectively, by $\mathbf{Z}^*$ and γ^*. Then, in step 3, the constraints of (34) will have at least one feasible set of variables for which $\gamma\leq\gamma^*$: $(\mathbf{L}^{(k-1)},\mathbf{Z}^*,\gamma^*)$. The same reasoning can be applied to show that the value of γ computed in (33) is, at most, the value of γ found in step 3 of the previous iteration and, as such, γ is non-increasing over the run of the algorithm.

5. SIMULATION RESULTS

This section presents the results of simulations that were carried out in order to assess the performance of the proposed decentralized state observers. Two similar formation structures were considered, with associated graphs depicted in Fig.2. The key difference between both is that,

Table 1. Algorithm for H_2 norm minimization

1) Initialization: set $k=1$; find $\mathbf{L}^{(0)}$ such that $(\mathbf{A}_g-\mathbf{L}^{(0)}\mathbf{C}_g)$ is stable (this can be done following, e.g., Theorem 1); choose a stopping criterion for the algorithm (e.g. a fixed number of steps, or a minimum improvement on the value of γ at each iteration).

2) Solve the optimization problem with LMI constraints

$$\begin{aligned} \min_{\substack{\mathbf{P}^{(k)}\in\mathbb{R}^{nN\times nN}\\ \mathbf{Z}\in\mathbb{R}^{nN\times nN}\\ \gamma\in\mathbb{R}^+}} \quad & \gamma \\ \text{subject to:} \quad & \mathbf{P}^{(k)}\succ\mathbf{0}, \\ & \mathbf{X}(\mathbf{P}^{(k)},\mathbf{L}^{(k-1)},\gamma)\prec 0, \\ & \begin{bmatrix}\mathbf{P}^{(k)} & \mathbf{I}\\ \mathbf{I} & \mathbf{Z}\end{bmatrix}\succ\mathbf{0}, \\ & \text{and trace}(\mathbf{Z})<\gamma. \end{aligned} \tag{33}$$

3) Solve the optimization problem with LMI constraints

$$\begin{aligned} \min_{\substack{\mathbf{L}^{(k)}\in\mathbb{R}^{nN\times 3M}\\ \mathbf{Z}\in\mathbb{R}^{nN\times nN}\\ \gamma\in\mathbb{R}^+}} \quad & \gamma \\ \text{subject to:} \quad & \mathbf{X}(\mathbf{P}^{(k)},\mathbf{L}^{(k)},\gamma)\prec 0, \\ & \begin{bmatrix}\mathbf{P}^{(k)} & \mathbf{I}\\ \mathbf{I} & \mathbf{Z}\end{bmatrix}\succ\mathbf{0}, \\ & \text{trace}(\mathbf{Z})<\gamma, \\ & \text{and } \mathbf{L}^{(k)}_{ij}=0 \text{ if } \mathbf{S}'_{ij}\neq 1, \\ & \forall i\in\{1,2,\ldots,nN\}, j\in\{1,2,\ldots,3M\}. \end{aligned} \tag{34}$$

4) If the stopping criterion is met, stop and take $\mathbf{L}^{(k)}$ as the gain for the decentralized state observer. Otherwise, set $k=k+1$ and go to step 2.

while graph (a) is acyclic, graph (b) has two additional edges that render it cyclic. The results are divided in two parts. In the first one, the algorithm proposed in the previous section is used for the two different formation structures, using in each case several distinct initial values for $\mathbf{L}$, which were found using Theorem 1. The second part takes the best gain $\mathbf{L}$ found for each formation structure and compares their performance in simulation.

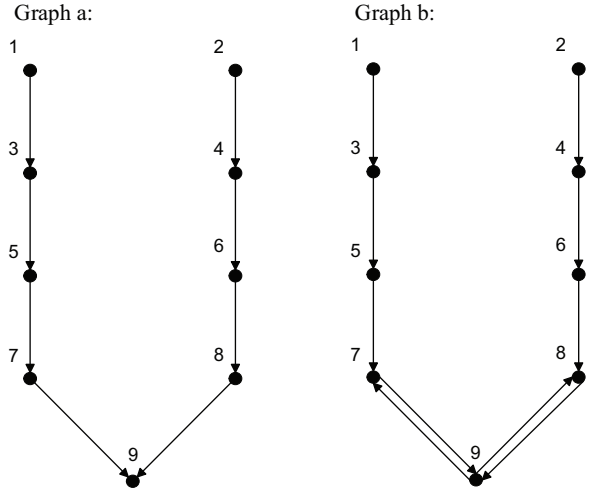

Fig. 2. Digraphs associated with the agent formations considered in simulation

5.1 H_2 Norm Minimization

To optimize the state observer gains, the process and observation noise must first be characterized. In the simulations, the linear acceleration, relative position, and absolute position measurements were corrupted by additive, uncorrelated, zero-mean white gaussian noise, with standard deviations of 0.01 (m/s^2), 1 (m), and 0.1 (m), respectively. Following this, $\mathbf{Q}$ and $\mathbf{R}$ were set to

$$\begin{cases} \mathbf{Q} = \text{diag}\,(0.0001,\ 0.0001,\ \ldots,\ 0.0001) \\ \mathbf{R} = \text{diag}\,(\mathbf{R}_0,\ \mathbf{R}_0,\ \mathbf{R}_1,\ \mathbf{R}_1,\ \mathbf{R}_1,\ \ldots,\ \mathbf{R}_1) \end{cases},$$

where $\mathbf{R}_0 = \text{diag}\,(0.01,\ 0.01,\ 0.01)$ refers to the absolute position measurements of agents 1 and 2, while $\mathbf{R}_1 = \mathbf{I}$ refers to the relative position measurements available to the other agents.

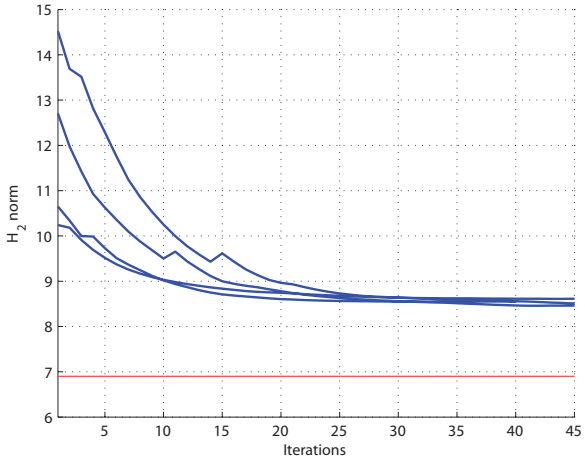

Fig. 3. Evolution of the algorithm for different initial conditions, acyclic graph. In red, H_2 norm of the ideal centralized filter

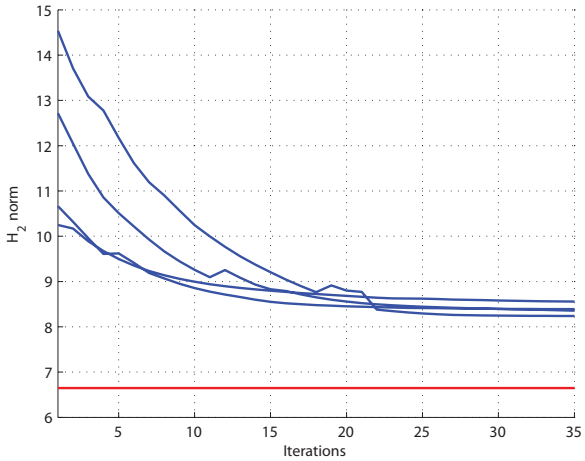

Fig. 4. Evolution of the algorithm for different initial conditions, cyclic graph. In red, H_2 norm of the ideal centralized filter

Fig. 3 and Fig. 4 depict the evolution of the H_2 cost during the optimization algorithm for the acyclic and cyclic graph, respectively, with 4 distinct initial values of $\mathbf{L}$. The lines in red represent the H_2 norm of the optimal centralized filter, whose gains were computed using classical Kalman filtering theory, see Jazwinski (1970). To complement the graphical data, Table 2 details the best values found in each case, and also the H_2 norm of the optimal centralized filter, to provide a comparison term. The results show that, in every case, the algorithm improved on the initial $\mathbf{L}$ and that, in the cyclic case, it used the additional edges constructively and it achieved better values than in the acyclic one. Note that, in the decentralized case, the agents have access to only a small fraction of the measurements made by the whole formation, so it would be unreasonable to expect the decentralized state observer to attain the performance of the optimal centralized one. Nevertheless, the performances that are achieved with the distributed solutions are very good considering the overwhelming communication and computational costs of the centralized filter.

Remark 3. As it was discussed in the previous section, theoretically, the value of γ is non-increasing over the run of the algorithm. However, Fig. 3 and Fig. 4 show a few outliers where the H_2 norm increases. This is due to numerical imprecisions in the solvers used to find solutions for (33) and (34).

Table 2. Lowest value achieved for γ

	Acy./Decent.	Acy./Cent.	Cyc./Decent.	Cyc./Cent.
γ_{min}	8.459	6.901	8.236	6.648

5.2 Performance assessment and comparison

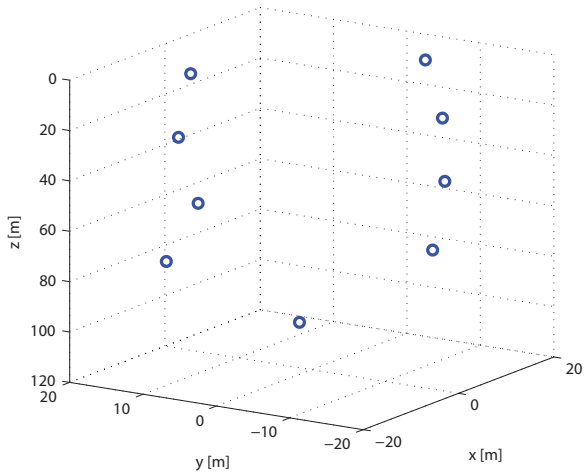

Fig. 5. Initial positions of the agents

The agents were distributed spatially replicating the drawing of the formation graph. Their initial positions are depicted in Fig. 5, and their initial velocity was set to zero for all coordinates. The system input, that is, the linear acceleration of the agent expressed in inertial coordinates, was set for each agent following the rule

$$\begin{cases} a_x(t) = A_x \dfrac{(2\pi)^2}{T_x^2} \cos\left(\dfrac{2\pi}{T_x} t + 2k_x\pi\right) \ \ (m/s^2) \\ a_y(t) = A_y \dfrac{(2\pi)^2}{T_y^2} \cos\left(\dfrac{2\pi}{T_y} t + 2k_y\pi\right) \ \ (m/s^2) \\ a_z(t) = 10 + A_z \dfrac{(2\pi)^2}{T_z^2} \cos\left(\dfrac{2\pi}{T_z} t + 2k_z\pi\right) \ \ (m/s^2) \end{cases}, \tag{35}$$

where the real scalars A_x, A_y, A_z, T_x, T_y, T_z, k_x, k_y and k_z were chosen arbitrarily for each agent picking values from the sets

$$\begin{cases} \{.5,\ 1,\ 1.5,\ 2\} & \text{for the As,} \\ \{20,\ 50,\ 80,\ 100\} & \text{for the Ts,} \\ \{0,\ .5,\ 1,\ 1.5\} & \text{for the ks.} \end{cases}$$

As for the local observers, and also the centralized Kalman filter, the initial values for all state estimates were set to zero, except for the ones corresponding to the acceleration of gravity. As $\mathbf{g}$ is known approximately, it was set to its real value in all estimators.

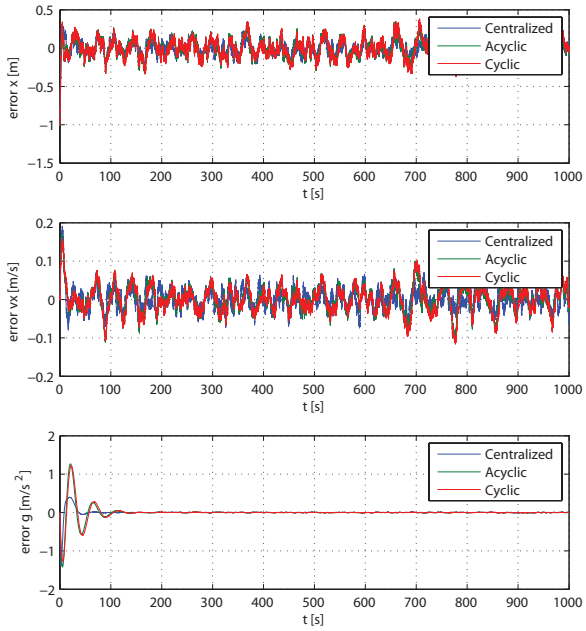

Fig. 6. Evolution of the estimation error of agent 9, for the optimal centralized Kalman filter and both decentralized state observers

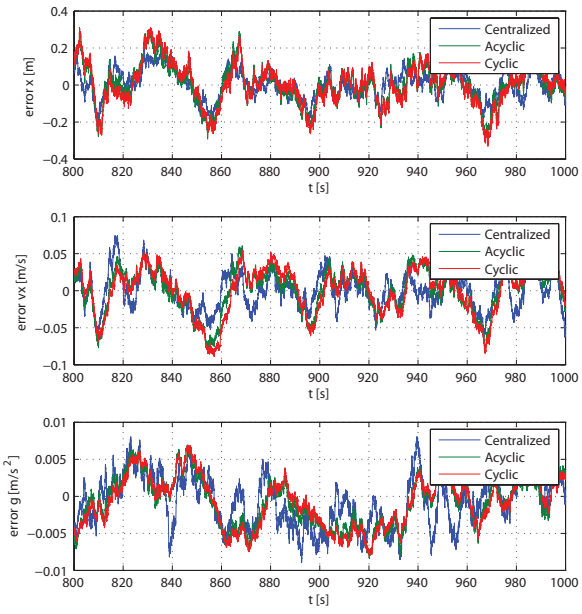

Fig. 7. Steady-state estimation error of agent 9, for the optimal centralized Kalman filter and both decentralized state observers

Table 3. Comparison of steady-state error standard deviation

	Decent./Acy.	**Decent./Cyc.**	**Cent./Cyc.**
σ_7^x	1.213×10^{-1}	1.155×10^{-1}	8.026×10^{-2}
σ_7^{vx}	3.558×10^{-2}	2.955×10^{-2}	2.373×10^{-2}
σ_7^g	4.118×10^{-3}	3.050×10^{-3}	3.735×10^{-3}
σ_8^x	1.272×10^{-1}	1.195×10^{-1}	8.087×10^{-2}
σ_8^{vx}	3.511×10^{-2}	2.940×10^{-2}	2.422×10^{-2}
σ_8^g	4.209×10^{-3}	3.148×10^{-3}	3.738×10^{-3}
σ_9^x	1.127×10^{-1}	1.163×10^{-1}	8.110×10^{-2}
σ_9^{vx}	2.964×10^{-2}	3.198×10^{-2}	2.404×10^{-2}
σ_9^g	3.960×10^{-3}	3.959×10^{-3}	3.952×10^{-3}

The results of the simulation are depicted in Fig. 6, Fig. 7 and Table 3. Fig. 6 shows the evolution of some of the error variables, namely for the first coordinate of the position and velocity, and the third coordinate of $\mathbf{g}$, of agent 9. As it can be seen, the error of both decentralized state observers converges to the vicinity of zero (they do not converge to zero only due to the presence of noise). Fig. 7 details the steady-state behavior of the error variables, after the initial transient has settled. To complement the graphical data, Table 3 compares the standard deviation of selected error variables for both filters and also the optimal centralized one, namely the first coordinate of the position and velocity, and the third coordinate of $\mathbf{g}$, of agents 7, 8, and 9, as those are the ones affected by the additional edges in the cyclic graph. As the data shows, while the performance is marginally worse in agent 9 for the state observer built on the cyclical graph, there is a clear improvement for agents 7 and 8. The performance of both decentralized filters is worse than that of the optimal centralized filter, which is to be expected given the vastly inferior amount of information available to estimate the state of each individual agent. Nevertheless, the overall results are quite satisfactory for the decentralized estimation structure, which evidences the goodness of the proposed distributed solutions in comparison with the heavy computational and communication loads of the centralized estimator.

6. CONCLUSIONS

The problem of decentralized state estimation in formations of AUVs was addressed in this paper. A method for designing local state observers presenting global error dynamics that converge globally asymptotically to zero was derived, and an algorithm for improving its H_2 nominal performance in the presence of noisy measurements or cycles in the graph associated with the formation was detailed. Finally, simulation results were presented that illustrate the performance of the proposed solution in noisy environments and the improvement resulting from the constructive use of additional measurements which render the formation graph cyclic.

REFERENCES

Astrom, K.J. and Murray, R.M. (2008). *Feedback Systems: An Introduction for Scientists and Engineers*. Princeton University Press.

Barooah, P. (2007). *Estimation and Control with Relative Measurements: Algorithms and Scaling Laws*. Ph.D. thesis, University of California, Santa Barbara.

Batista, P., Silvestre, C., and Oliveira, P. (2009a). Position and Velocity Optimal Sensor-based Navigation Filters for UAVs. In *Proceedings of the 2009 American Control Conference*, 5404–5409. Saint Louis, USA.

Batista, P., Silvestre, C., and Oliveira, P. (2010). A Sensor-b ased Long Baseline Position and Velocity Navigation Filter for Underwater Vehicles. In *Proceedings of the 8th IFAC Symposium on Nonlinear Control Systems - NOLCOS 2010*, 302–307. Bologna, Italy.

Batista, P., Silvestre, C., and Oliveira, P. (2009b). Single Range Navigation in the presence of Constant Unknown Drifts. In *Proceedings of the European Control Conference 2009*, 3983–3988. Budapest, Hungary.

Bender, J. (1991). An overview of systems studies of automated highway systems. *IEEE Transactions on Vehicular Technology*, 40(1), 82–99.

Curtin, T.B., Bellingham, J.G., and Webb, D. (1993). Autonomous Oceanographic Sampling Networks. *Oceanography*, 6, 86–94.

Fax, J.A. (2002). *Optimal and Cooperative Control of Vehicle Formations*. Ph.D. thesis, California Institute of Technology.

Fransson, C. and Lennartson, B. (2003). Low order multicriteria H_∞ design via bilinear matrix inequalities. In *Proceedings of the 42nd IEEE Conference on Decision and Control*, volume 5, 5161–5167.

Giulietti, F., Pollini, L., and Innocenti, M. (2000). Autonomous formation flight. *IEEE Control Systems Magazine*, 20(6), 34–44.

Healey, A. (2001). Application of formation control for multi-vehicle robotic minesweeping. In *Proceedings of the 40th IEEE Conference on Decision and Control*, volume 2, 1497–1502.

Jazwinski, D.B. (1970). *Stochastic Processes and Filtering Theory*. Academic Press.

Middleton, R.H. and Braslavsky, J.H. (2010). String Instability in Classes of Linear Time Invariant Formation Control With Limited Communication Range. *IEEE Transactions on Automatic Control*, 55(7), 1519–1530.

Scherer, C. and Weiland, S. (2005). *Linear Matrix Inequalities in Control*.

Sousa, R., Oliveira, P., and Gaspar, T. (2009). Joint Positioning and Navigation Aiding Systems for Multiple Underwater Robots. In *8th IFAC Conference on Manoeuvring and Control of Marine Craft-MCMC 2009*, 167–172. Guaruja, Brazil.

Toker, O. and Ozbay, H. (1995). On the NP-hardness of solving bilinear matrix inequalities and simultaneous stabilization with static output feedback. In *Proceedings of the American Control Conference, 1995*, volume 4, 2525–2526.

Tsitsiklis, J.N. (1984). *Problems in Decentralized Decision Making and Computation*. Ph.D. thesis, Massachusetts Institute of Technology.

Wallis, W.D. (2007). *A Beginner's Guide to Graph Theory*. Birkhauser, 2nd edition.

West, D.B. (2001). *Introduction to Graph Theory*. Pearson, 2nd edition.

Wolfe, J.D., Chichka, D.F., and Speyer, J.L. (1996). Decentralized Controllers for Unmanned Aerial Vehicle Formation Flight. In *Proceedings of AIAA Conference on Guidance, Navigation, and Control*.

Yanakiev, D. and Kanellakopoulos, I. (1996). A Simplified Framework for String Instability Analysis in AHS. In *Proceedings of the 13th IFAC World Congress*, volume Q, 177–182. San Francisco, CA, USA.